Available online at www.sciencedirect.com
SCIENCE DIRECT®
Journal of Magnetic Resonance 176 (2005) 234–238
JMR Journal of Magnetic Resonance
www.elsevier.com/locate/jmr

Communication

# Selecting ordered environments in NMR of spin 3/2 nuclei via frequency-sweep pulses

Wen Ling, Alexej Jerschow *

*Department of Chemistry, New York University, 100 Washington Square East, New York, NY 10003, USA*

Received 9 May 2005; revised 10 June 2005
Available online 18 July 2005

**Abstract**

We demonstrate that frequency-swept pulses can be used for the selective and enhanced detection of quadrupolar nuclei located in anisotropic environments. The primary driving force for this technique development is the field of sodium-MRI, where sodium signals from locally ordered environments are known to be diagnostic of cartilage defects. We demonstrate here simple one-dimensional images of model systems, in which the signals from free sodium ions are suppressed, while ordered sodium is detected via the narrow central transition signal.


*Keywords:* Sodium MRI; Contrast mechanism; Double-quantum filter; Satellite transitions; Quadrupolar coupling; Double-frequency sweep

## 1. Introduction

The $^{23}$Na nucleus has a spin of 3/2 and is subject to an electric quadrupolar interaction when located in an anisotropic environment, or when performing anisotropic motion (such as, for example, rotation around a large molecule with a preferred axis) [1]. Fox axial symmetry, the Hamiltonian for this interaction can be described by $H_Q = \omega_Q\left[3I_z^2 - I(I+1)\right]$, where $\omega_Q$ is the quadrupolar coupling constant, usually given in angular frequency units, or as $\omega_Q/2\pi$ in Hz. Its strength varies with the orientation of the electric field gradient (EFG) tensor with respect to the static magnetic field. The NMR spectrum of a single sodium atom in an anisotropic environment displays three resonances, located at the frequencies $-3\omega_Q/2\pi$, 0, and $3\omega_Q/2\pi$ relative to the isotropic chemical shift of the atom. In the case of a random collection of crystallites with different orientations of the EFGs with respect to the static magnetic field, the positions of the outer resonances (the satellite transitions) vary and a powder spectrum is obtained [2]. The same situation occurs when the sodium ions are moving (anisotropically) around an axis, determined by their association with macromolecular structures, such as the proteoglycan-collagen systems in cartilage tissue [1]. The central transition ($-1/2 \rightarrow 1/2$) does not experience any orientational dependence and stays narrow, except for very large quadrupolar coupling constants, which typically only arise in solid systems [3].

Sodium concentrations monitored in cartilage tissue by $^{23}$Na-MRI show a strong correlation with charge densities and thereby proteoglycan content [4]. Proteoglycan depletion is accompanied by a decrease in sodium concentration [5]. This has been demonstrated both in in vivo models [6,7] and in vivo [8–10]. Another example of the application of $^{23}$Na-MRI is the study of brain tumors [11]. Distinguishing between free sodium and sodium associated with macromolecules provides strong diagnostic power for cartilage and other tissue pathologies [12,13]. Other areas of applications include such experiments in mitochondrial suspensions [14], the study of the effect of the cytoskeleton formation on the anisotropic motion in red blood cells [13], and the study of the

* Corresponding author.
*E-mail address:* alexej.jerschow@nyu.edu (A. Jerschow).

1090-7807/$ - see front matter © 2005 Elsevier Inc. All rights reserved.
doi:10.1016/j.jmr.2005.06.006

competition between $Na^+$ and $Li^+$ for the unsealed and cytoskeleton-depleted human red blood cell membrane [15].

The central transition of ordered sodium overlaps frequently with the signal arising from free sodium. Chemical shift reagents may help to distinguish, for example, intracellular from extracellular sodium [16,17]. On the other hand, only the ordered sodium exhibits a quadrupolar interaction and therefore broadened satellite-transition signals [18]. Techniques have been developed that allow one to selectively observe the signals from ordered environments, i.e., from those ions that exhibit a non-vanishing quadrupolar interaction [1,12,18]. These experiments are best described using spherical tensor operators [1,12,19,20]. After a hard 90° pulse the magnetization can be written in terms of the transverse magnetization components $T^1_{\pm1}$, which represent spherical tensor operators of rank one and order plus or minus one. In general, one distinguishes between two scenarios for their time evolution. Under the action of the quadrupolar Hamiltonian this operator transforms into a mixture of $T^2_{\pm1}$. These terms can be converted into double quantum coherence, $T^2_{\pm2}$. A double-quantum filter experiment selects the signals arising from ordered sodium.

On the other hand, ions that experience slow isotropic motion, may also contribute to a double-quantum signal, via a relaxation-induced pathway symbolized by $T^1_{\pm1} \rightarrow T^3_{\pm1} \rightarrow T^3_{\pm2}$ [1]. The spectroscopic signature of this signal can in some cases be distinguished from the former [1,12]. Specialized pulse sequences can further minimize the appearance of the free sodium signals [1,12].

The modified Jeener–Broekaert experiment [1] selects the signals of ordered-sodium ions using a $z$-filter. The coherence transfer in this experiment can be described by the following trajectory: $T^1_{\pm1} \rightarrow T^2_{\pm1}$, $T^3_{\pm1} \rightarrow T^2_0 \rightarrow T^2_{-1} \rightarrow T^1_{-1}$ (the $T^3_{\pm1}$ components cancel each other by applying the $z$-filter). The advantage of this sequence is that the selection of $T^2_0$ over $T^3_0$ is relatively insensitive to $B_1$ field inhomogeneities. However, as Navon et al. [12] pointed out, and we noticed in testing this sequence, the leakage due to $T^1_0$ may be problematic. Therefore, the appearance of the free sodium signal may hamper its applicability.

The double-quantum sequence selects the coherence corresponding to ordered ions solely by the flip-angle setting, and it is therefore extremely sensitive to $B_1$ field in homogeneity. Leakage of the $T^3_{\pm2}$ term often occurs. Another disadvantage of both sequences is that since the lineshape of the filtered component is dispersive, it is not a desirable method for imaging purposes, especially when a broad distribution of quadrupolar coupling constants is present.

A marked improvement of above methods was originally developed by Wimperis and colleagues [1], in which the coherence present in the satellite transitions is transferred into the central transition, via a double Jeener–Broekaert experiment. The advantage of this sequence is that the signal from ordered sodium may be converted into a central transition component with a large signal-to-noise ratio due to a narrow lineshape. Unfortunately, the aforementioned disadvantages of the Jeener–Broekaert sequence also apply here.

Recently, a relatively simple approach was described that allows one to suppress the central transition signals using two soft pulses [18], but the back-transfer into the central transition was not developed.

The experiment demonstrated here represents an alternative to the methods mentioned above. We note that it is often possible to adjust this method such that the satellite transitions do not appear in the spectrum at all. This has a marked resolution advantage in imaging as shown below. Another advantage is its potential for $B_1$ robustness, as it does not rely on precise flip-angle settings.

## 2. Experimental

All experiments were performed on a Bruker Avance 500 MHz spectrometer with a BBI probe tuned to the sodium frequency, equipped with a single-axis gradient accessory with a maximum strength of 50 G/cm. Two samples with different residual quadrupolar coupling constants (QCC) were prepared.

### 2.1. Sample A

Liquid-crystalline system formed by a mixture of 37.9 wt% sodium decyl sulfate, 6.7 wt% decanol, and 55.4 wt% $H_2O$ at 25 °C. The mixture gives rise to a residual quadrupolar splitting of approximately 8.5 kHz for the sodium signal.

### 2.2. Sample B

Liquid-crystalline system formed by a mixture of 36 wt% sodium decyl sulfate, 7.2 wt % decanol, and 57 wt% $H_2O$ at 20 °C. The mixture gives rise to a residual quadrupolar splitting that peaks around 3.5 kHz for the sodium signal.

The double-frequency-sweep (DFS) pulses were created according to $\omega_1(t) = \omega_1 \cos[\omega_1 t - (\omega_s - \omega_f)t^2/2\tau]$, where $\omega_1$ is the overall rf-field, $\omega_s$ and $\omega_f$ are the start and final sweep frequencies, and $\tau$ is the duration of the pulse.

The phase cycle for the sequences shown in Fig. 1 was as follows: $\phi(\text{CTsat}) = m \times 90°$, $\phi(\text{DFS}) = l \times 90°$, the hard pulse phase $= k \times 90°$, and the receiver phase $\varphi_R = k \times 90°$, where $m$, $k$, and $l$ assume the values {0,1,2,3} independently. The parameters of the soft pulse were $\omega_1/2\pi = 200$ Hz, pulse length 1140 μs, and

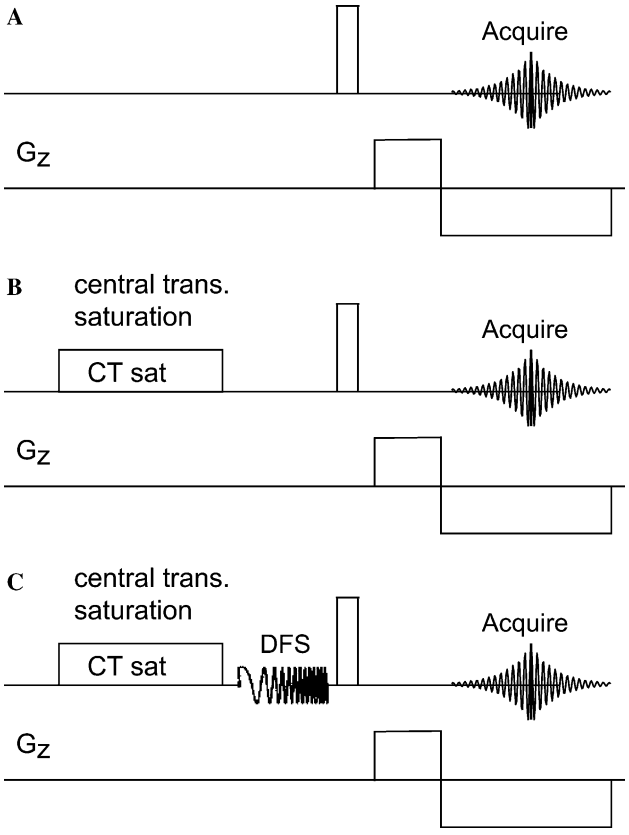


Fig. 1. Pulse sequences used in this study. (A) Simple pulse gradient echo experiment, (B) as in (A) but with saturation of the central transition via a weak rf-irradiation (CTsat), (C) as in (B) but with a double-frequency-sweep (DFS) pulse to transfer the populations from the satellite to the central transitions.

for the hard pulse, $\omega_1/2\pi = 22$ kHz, pulse length 3.6 μs. All DFS pulses had a power of $\omega_1/2\pi = 2$ kHz and durations of 400 μs. The sweep was from 1.8 to 10 kHz, for both samples. For the 1D imaging profile, the gradient strength for sample A was 4 G/cm, while that for sample B was 8 G/cm. The gradient echo time was 1 ms. 2048 sample points were acquired to cover a spectral window of 50 kHz.

The $T_1$ relaxation constants were measured using an inversion recovery sequence, and the $T_2$ constants were measured using the CPMG sequence with $\tau = 20$, 50, and 70 μs delays between the refocusing pulses (90° pulse duration 12.3 μs). The relaxation data are summarized in Table 1.

Table 1
$T_1$ and $T_2$ data

| | $T_1$ (central) [ms] | $T_1$ (satellite) [ms] | $T_2$ ($\tau = 20$ μs) [ms] | $T_2$ ($\tau = 50$ μs) [ms] | $T_2$ ($\tau = 70$ μs) [ms] |
|---|---|---|---|---|---|
| Sample A | 14.1 | 14.0 | 10.3 | 9.6 | 13.2 |
| Sample B | 13.3 | 12.7 | 9.9 | 9.1 | 7.2 |

$T_1$ is reported for both the central and the satellite transitions. $T_2$ is reported at different delay times of the CPMG sequence.

## 3. Results and discussion

We demonstrate the new contrast method in the following way: first, we need to suppress the signal from free sodium environments. This can be done in the form of a long and weak rf-irradiation. A so-called CPS sequence was reported previously to perform this task [18]. Ideally, the central transition saturation pulse creates a density matrix of the form

$$\begin{pmatrix} -3/2 & & & \\ & 0 & & \\ & & 0 & \\ & & & 3/2 \end{pmatrix} = \frac{9}{10}T_0^1 + \frac{1}{\sqrt{10}}T_0^3. \quad (1)$$

A 90° hard pulse would, however, create both satellite and central transition coherences. In the CPS sequence, both the soft irradiation on the central transition and the hard pulse flip angle are varied to avoid this problem [18]. As a result, in an optimal setting, neither pulse is a 90° pulse. It can be shown that as the hard pulse flip angle increases, the soft pulse flip angle needs to be increased. According to Navon et al. [18] the maximum hard pulse flip angle at which central transition suppression is achieved is 41.8°. While this procedure in general incurs a loss of sensitivity of approximately 10% as compared to a 90° pulse experiment a clean removal of the central transition (and free sodium) signals is possible [18].

We combine this two-pulse CPS sequence with a double-frequency-sweep (DFS) pulse in between the central transition saturation (CTsat) pulse and the hard pulse. The DFS pulses are used to convert the populations encoded in the satellite transitions into central transition populations for detection [21–24]. The DFS pulses work best in a regime described as adiabatic, in which the effective rf-field is large compared to the sweep speed [22]. Such a regime, however, is often difficult to achieve when the quadrupolar couplings are small. Furthermore, adiabaticity considerations are strictly valid only in cases when multiple level anti-crossings do not occur simultaneously. On the other hand, adiabaticity is not a requirement for achieving coherence transfers, rather it is a guiding principle for specific situations. As the parameters show, the DFS pulses used here are not performed under adiabatic conditions. In cartilage samples, where the quadrupolar coupling constants are smaller than in the samples studied here, the adiabatic regime may dictate relatively slow sweep speeds, in which case much of the magnetization will be lost due to relaxation. Under conditions of controlled violation of adiabaticity, however, faster experiments with smaller relaxation losses become possible. The theoretical description of this process is complicated, and perhaps, little insightful as several level crossings and anti-crossings happen almost

simultaneously. We adjust the pulse power and sweep speed such that the satellite transitions appear saturated at the same time as the populations are transferred to the central transition. This has the additional benefit of reducing satellite image artifacts. The DFS parameters are further adjusted to recover a maximum of signal intensity in the central transition.

To demonstrate the stages of the coherence transfer we perform three different experiments (Fig. 2), both without and with imaging gradients for both samples. The first experiment is a simple hard-pulse experiment (sequence of Fig. 1A), all three transitions are present, as well as all three components of the one-dimensional image (Figs. 2A, D, G, and J). The second experiment is a hard-pulse experiment with saturation of the central transition, to remove the signal from free sodium (sequence of Fig. 1B). The corresponding spectra are shown in Figs. 2B, E, H, and K, and one can see that the central transition resonance, as well as the central transition image are removed. The third experiment is a saturation—DFS—hard-pulse experiment, in which the central transition reappears as a result of the transfer of the populations from the satellite transitions (sequence of Fig. 1C). The corresponding spectra are shown in Figs. 2C, F, I, and L. As is particularly evident in Fig. 2K, the presence of the satellite transitions significantly perturbs the image due to the overlapping satellite-transition signals. If these are removed and their magnetization is transferred into the central transition, the image appears much cleaner (as shown in Fig. 2L). We note that spikes appear in the images of Figs. 2D, E, and F at the edges of the images towards the edges of the rf-coil where the field falls off to zero.

After applying the DFS in addition to central transition suppression the recovered central transition peak appears at an intensity of 61% for sample A, and 78% for sample B with respect to the original central transition peak. This demonstrates that we are able to observe the ordered sodium signals with relatively large efficiency even though the DFS pulses are far from being adiabatic. Relaxation effects (Table 1) can be neglected for the samples studied, however, as was mentioned above, it is important to be able to perform these pulse sequences within very short time intervals, as in cartilage samples the estimated relaxation losses would exceed the losses incurred due to non-ideal pulses. We also observe an increase in the satellite-transition signals by a factor of 1.4 after the central transition suppression step, more than observed in the original CPS experiment in Fig. 4 of Ref. [18]. We are working to optimize the components of this new sequence to increase further the overall efficiency.

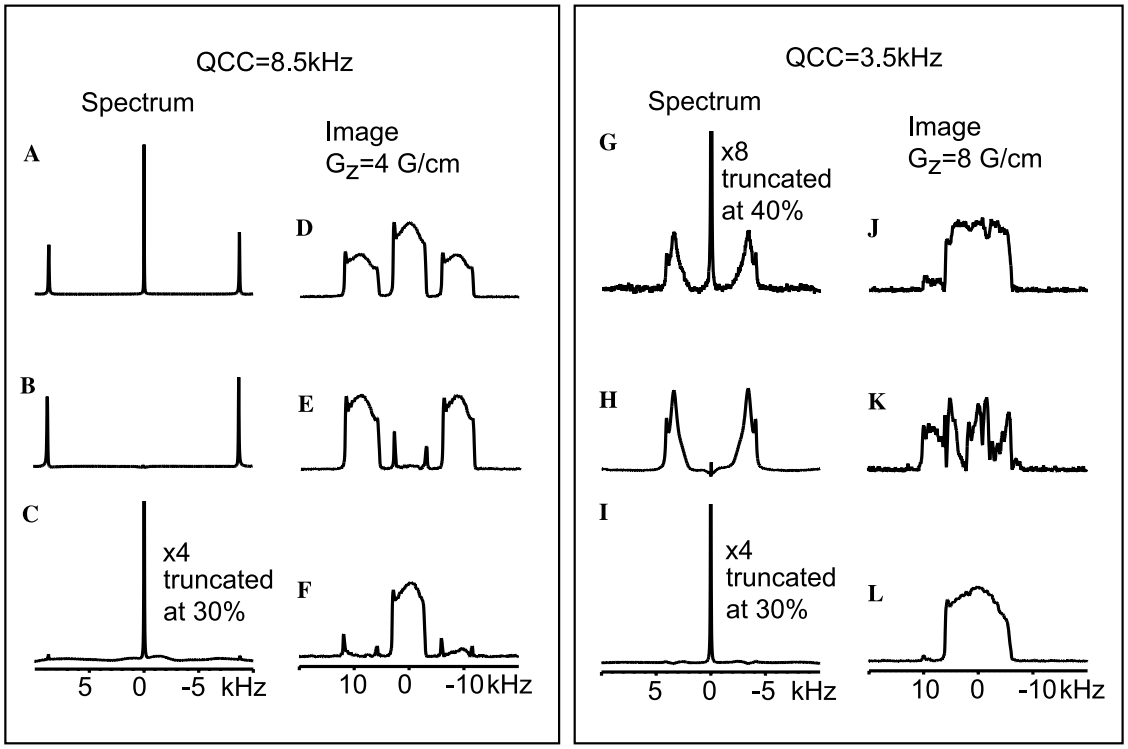


Fig. 2. Spectra and one-dimensional images on samples A and B. The simple pulse experiments of Fig. 1A are shown in (A), (D), (G), and (J), each acquired both with (D and J) and without (A and G) the gradient echo sequence. The experiments of Fig. 1B are shown in (B), (E), (H), and (K), each acquired both with (E and K) and without (B and H) the gradient echo sequence. The experiments of Fig. 1C are shown in (C), (F), (I), and (L), each acquired both with (F and L) and without (C and I) the gradient echo sequence. All spectra were acquired using an accumulation of 64 transients, except the one in Figure (G), where only one transient was used.

## 4. Conclusions

We demonstrate how signals from sodium in anisotropic environments can be observed selectively by the use of DFS pulses, while the signals from isotropic sodium can be suppressed. This technique is akin in function to the previously described double-quantum filtered or Jeener–Broeckaert sequences, however, with the additional benefits of the removal of the satellite transitions, the observation of the in-phase central transition component, and the relative robustness against $B_1$ inhomogeneity artifacts, which is generally afforded by frequency-sweep pulses. It also contains adjustable parameters that allow one to tune it to certain frequency ranges for the DFS transfer. Using this property one can adjust the image contrast mechanism to visualizing a certain degree of order in the tissue. Experiments that demonstrate such selectivity are underway, as are numerical optimizations that make these types of sequences applicable to samples with quadrupolar splittings smaller than the ones shown in this paper.

## Acknowledgments

We acknowledge funds from the NYU Whitehead Fellowship for Junior Faculty in the Biological and Biomedical Sciences. NYU's NMR facilities were supported by a NSF Grant MRI-0116222. We acknowledge support by Dr. Chin Lin and the Molecular Imaging and Contrast Agent Working Group at NYU, as well as, stimulating discussions with Dr. Gil Navon, Dr. Uzi Eliav, and Dr. Philip W. Kuchel.

## References

[1] R. Kemp-Harper, S.P. Brown, C.E. Hughes, P. Styles, S. Wimperis, $^{23}$Na NMR methods for selective observation of sodium ions in ordered environments, Prog. Nucl. Magn. Reson. Spectrosc. 30 (1997) 157–181.

[2] D.D. Laws, H.M.L. Bitter, A. Jerschow, Solid-state NMR methods in chemistry, Angew. Chem. Intl. Ed. Engl. 41 (2002) 3096–3126.

[3] A. Jerschow, From nuclear structure to the quadrupolar NMR interaction and high-resolution spectroscopy, Prog. Nucl. Magn. Reson. Spectrosc. 46 (2005) 63–78.

[4] E.M. Shapiro, A. Borthakur, A. Gougoutas, R. Reddy, Na-23 MRI accurately measures fixed charge density in articular cartilage, Magn. Reson. Med. 47 (2002) 284–291.

[5] A. Borthakur, E.M. Shapiro, J. Beers, S. Kudchodkar, J.B. Kneeland, R. Reddy, Sensitivity of MRI to proteoglycan depletion in cartilage: comparison of sodium and proton MRI, Osteoarthritis Cartilage 8 (2000) 288–293.

[6] A.J. Wheaton, A. Borthakur, G.R. Dodge, B. Kneeland, H.R. Schumacher, R. Reddy, Sodium magnetic resonance imaging of proteoglycan depletion in an in vivo model of osteoarthritis, Acad. Radiol. 11 (2004) 21–28.

[7] A.J. Wheaton, A. Borthakur, E.M. Shapiro, R.R. Regatte, S.V.S. Akella, J.B. Kneeland, R. Reddy, Proteoglycan loss in human knee cartilage: quantitation with sodium MR imaging—feasibility study, Radiology 231 (2004) 900–905.

[8] A. Borthakur, E.M. Shapiro, S.V.S. Akella, A. Gougoutas, J.B. Kneeland, R. Reddy, Quantifying sodium in the human wrist in vivo by using MR imaging, Radiology 224 (2002) 598–602.

[9] E.K. Insko, D.B. Clayton, M.A. Elliott, In vivo sodium MR imaging of the intervertebral disk at 4 T, Acad. Radiol. 9 (2002) 800–804.

[10] R. Reddy, E.K. Insko, E.A. Noyszewski, R. Dandora, J.B. Kneeland, J.S. Leigh, Sodium MRI of human articular cartilage in vivo, Magn. Reson. Med. 39 (1998) 697–701.

[11] R. Ouwerkerk, K.B. Bleich, J.S. Gillen, M.G. Pomper, P.A. Bottomley, Tissue sodium concentration in human brain tumors as measured with 23Na MR imaging, Radiology 227 (2003) 529–537.

[12] G. Navon, H. Shinar, U. Eliav, Y. Seo, Multiquantum filters and order in tissues, NMR Biomed. 14 (2001) 112–132.

[13] T. Knubovets, H. Shinar, U. Eliav, G. Navon, A Na-23 multiple-quantum-filtered NMR study of the effect of the cytoskeleton conformation on the anisotropic motion of sodium ions in red blood cells, J. Magn. Reson. B 110 (1996) 16–25.

[14] S.M. Grieve, B. Wickstead, A.M. Torres, P. Styles, S. Wimperis, P.W. Kuchel, Multiple-quantum filtered 17O and $^{23}$Na NMR analysis of mitochondrial suspensions, Biophys. Chem. 73 (1998) 137–143.

[15] C. Srinivasan, N. Minadeo, J. Toon, D. Graham, D.M. de Freitas, C.F.G. Geraldes, Competition between $Na^+$ and $Li^+$ for unsealed and cytoskeleton-depleted human red blood cell membrane: a $^{23}$Na multiple quantum filtered and $^7$Li NMR relaxation study, J. Magn. Reson. 140 (1999) 206–217.

[16] I. Ronen, S.G. Kim, Measurement of intravascular $Na^+$ during increased CBF using Na-23 NMR with a shift reagent, NMR Biomed. 14 (2001) 448–452.

[17] C. Weidensteiner, M. Horn, E. Fekete, S. Neubauer, M. von Kienlin, Imaging of intracellular sodium with shift reagent aided $^{23}$Na CSI in isolated rat hearts, Magn. Reson. Med. 48 (2002) 89–96.

[18] U. Eliav, K. Keinan-Adamsky, G. Navon, A new method for suppressing the central transition in $I = 3/2$ NMR spectra with a demonstration for Na-23 in bovine articular cartilage, J. Magn. Reson. 165 (2003) 276–281.

[19] U. Eliav, G. Navon, Quadrupole-echo techniques in multiple-quantum-filtered NMR-spectroscopy of heterogeneous systems, J. Magn. Reson. A 115 (1995) 241–253.

[20] L. Tsoref, U. Eliav, G. Navon, Multiple quantum filtered nuclear magnetic resonance spectroscopy of spin 7/2 nuclei in solution, J. Chem. Phys. 104 (1996) 3463–3471.

[21] S. Vega, Y. Naor, Triple quantum NMR on spin systems with $I > 1/2$ in solids, J. Chem. Phys. 75 (1981) 75–86.

[22] E.V. van Veenendaal, B.H. Meier, A.P.M. Kentgens, Frequency stepped adiabatic passage excitation of half-integer quadrupolar spin systems, Mol. Phys. 93 (1998) 195–213.

[23] D. Iuga, H. Schafer, R. Verhagen, A.P.M. Kentgens, Population and coherence transfer induced by double frequency sweeps in half-integer quadrupolar spin systems, J. Magn. Reson. 147 (2000) 192–209.

[24] R. Kumar, W. Ling, W. Schoefberger, A. Jerschow, Separated quadrupolar field experiment, J. Magn. Reson. 172 (2005) 209–213.